Electronic Supplementary Information for

Transition of lithium growth mechanisms in liquid electrolytes

Peng Bai[a,*], Ju Li[b,c], Fikile R. Brushett[a], Martin Z. Bazant[a,d,e,*]

Departments of [a]Chemical Engineering, [b]Nuclear Science and Engineering, [c]Materials Science

and Engineering and [d]Mathematics, Massachusetts Institute of Technology, 77 Massachusetts

Avenue, Cambridge, MA 02139, USA

[e]Department of Materials Science and Engineering and SUNCAT Interfacial Science and

Catalysis, Stanford University, Stanford, CA 94305, USA

*Correspondence to: pengbai@mit.edu, bazant@mit.edu

This file includes:

Supplementary text with

Figs. S1 to S7

Tables S1 to S3

References (63-64)

Other Supplementary Materials for this manuscript includes the following:

Movies S1 to S7

Growth of mossy lithium before Sand's time
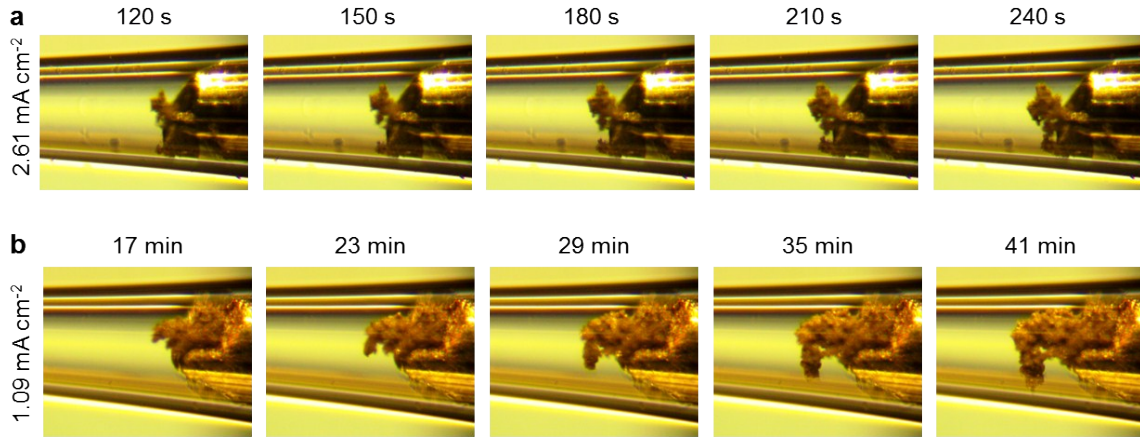
Figure S1. Visualization of the root-growth mechanism of mossy lithium before Sand's time. While the deposits continuously thicken themselves globally, the (a) displacement and (b) rotation of the tips reveal that major proliferations occur at locations behind the tips, which is a stark difference from existing models of transport-limited growth occurring only at the tips.

Calculation of the current densities

Since the Sand's time and the instability occurred on the surface of the electrode are all determined by the depletion of the electrolyte, the current density in Sand's formula should be the flux density through the cross-section of the capillary, not the local current density on the electrode, so we measured the inner diameter of the capillary to determine the area (Fig. S2), based on which current density is calculated.
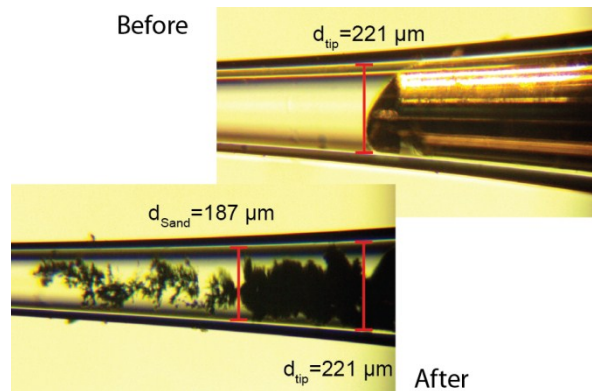
Figure S2. Example of the diameter measurement. J_{tip}=2.61 mA cm^{-2}

Table S1. Total current and the corresponding current density of the capillary cell experiments.

c_0 / mol l^{-1}	I / μA	d_{tip} / μm	d_{Sand} / μm	J_{tip} / mA cm^{-2}	J_{Sand} / mA cm^{-2}	J_{avg} / mA cm^{-2}	t_{Sand} / s
0.5	0.3	272	243	0.52	0.65	0.58	7953
	0.7	302	277	0.98	1.16	1.07	2750
	1.2	316	314	1.53	1.55	1.54	1500
	1.2	277	266	1.99	2.16	2.08	1130
	2	316	247	2.55	4.18	3.36	893
	2.6	286	277	4.05	4.32	4.18	530
	2.7	230	216	6.50	7.37	6.94	300
	5	252	228	10.03	12.25	11.14	235
1	0.5	242	181	1.09	1.94	1.52	6780
	0.7	229	191	1.70	2.44	2.07	5600
	1.4	287	253	2.17	2.79	2.48	3100
	1	221	187	2.61	3.64	3.13	2690
	1.4	251	213	2.83	3.93	3.38	2005
	2.6	321	263	3.21	4.79	4.00	1880
	2.5	266	240	4.50	5.53	5.01	1100
	4	291	249	6.02	8.22	7.12	730
	5.8	330	262	6.78	10.76	8.77	610
2	0.9	233	161	2.11	4.42	3.27	7986
	2	285	236	3.14	4.57	3.86	4055
	2.2	271	173	3.82	9.36	6.59	3537
	2.7	264	182	4.93	10.38	7.66	2224
	4.5	284	215	7.11	12.40	9.75	1316
	4	235	169	9.23	17.84	13.53	868
	7.5	277	207	12.45	22.30	17.37	664

The three kinds of current densities all produce similar scaling for each concentration. In this paper, we only use the one at the initial position of the electrode, i.e. J_{tip}, for all analyses.

Experimental Observation of Electro-osmotic Flow

While electro-osmotic (EO) flow is not significant in practical batteries using dense porous separators, the analysis presented here confirm that EO convection is the primary reason for the observed deviation from the theoretical scaling of Sand's time with current. Thanks to the small lithium debris produced during cell assembly, we are able to observe the fluid velocity in various locations of the capillary to obtain a rough estimation of the Peclet number, which measures the importance of convection relative to diffusion.
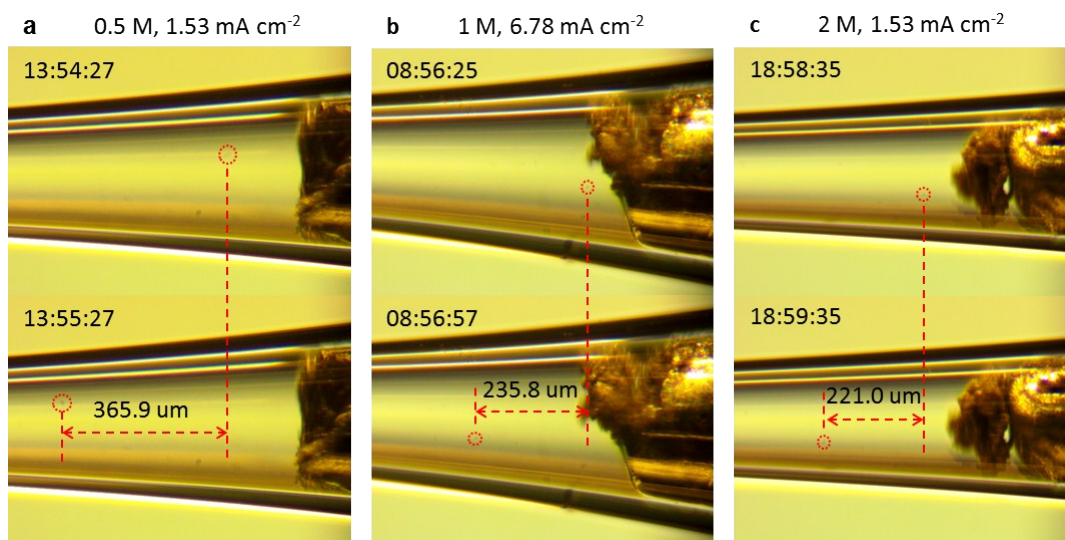
Figure S3. Estimation of the local fluid velocity from floating lithium debris in the capillaries. Also see movies S3-S5.

Table S2. Estimation of the experimental Peclet numbers.

c_0 (mole l^{-1})	J_{tip} (mA cm^{-2})	Δt (s)	ΔL (um)	U (um s^{-1})	d (um)	D (cm^2 s^{-1})	Pe=Ud/D
0.5	1.53	60	366	6.10	286	3.4×10^{-6}	5.13
1.0	6.78	32	236	7.38	330	3.0×10^{-6}	8.12
2.0	3.82	60	221	3.68	235	1.7×10^{-6}	5.09

For the above three experiments that most clearly show convection, the Peclet numbers based on direct observations of the fluid velocity are calculated in Table S2. Values larger than one indicate significant convection, which is neglected in the classical derivation of Sand's time.

Effects of Electro-osmotic Convection on the Apparent Diffusivity

Naively, convection would be expected to enhance mass transfer and thus increase Sand's time compared to pure diffusion, but the coupled problem of EO flow and concentration polarization is very complicated, even in steady state, and has never been analyzed under transient conditions. It is also possible that convective mixing will lower the local "bulk" concentration outside the diffusion layer, thus decreasing Sand's time, and increasing the apparent diffusivity from Sand's formula, as observed in our experiments discussed in the main text. Here, we briefly attempt to estimate the effect of EO convection on the apparent diffusivity from Sand's formula, just to show that this is a plausible explanation of the data, in light of the observed flows and Peclet numbers larger than one shown above.

EO flow in a closed capillary (or porous medium) leads to pressure-driven backflow, in order to maintain zero average flow rate. The sum of EO plug flow driven by the surface double layers and parabolic Poiseuille flow in the opposite direction yield vortices of flow, which have previously been observed in thin-gap (microfluidic) copper electrodeposition experiments by Huth et al.[45]. A simple theory to capture the effect of electro-osmotic convection on the effective diffusivity in a capillary based on Taylor dispersion has been proposed by Yaroshchuk et al.[63]:

$$\frac{D_{app}}{D_{app}^0} = 1 + \frac{1}{48}\mathrm{Pe}^2, \quad \mathrm{Pe} = \frac{\epsilon_0 \epsilon_r \zeta RJ}{\eta \sigma D_{app}^0}. \tag{S1}$$

where, $D_{app}^0 = D_{app}(J = 0)$ is a reference diffusivity at zero current and the Peclet number is estimated using the Helmholtz-Smoluchowski electro-osmotic slip formula and the mean electric field, equal to the current density divided by the mean local conductivity. Although this theory loses validity above the limiting current in a strongly depleted capillary[46, 63], it should suffice for our analysis of the current-dependence of Sand's time, prior to diffusion limitation and the onset of dendrites.

Following the suggestion of a recent numerical study[54], the apparent diffusivity in Sand's time for a concentrated electrolyte (without convection) may be approximated by using the traditional apparent diffusivity, e.g. measured by linear response to a small current step[42,43], evaluated at an intermediate concentration, such as $c_0/2$.

The electric field and resulting EO flow are the largest in the depleted region close to the electrode as Sand's time is approached, and this is where the strongest convection is observed in the experiments. Thus, we estimate the local conductivity in the EO Peclet number using 1/5 of the bulk salt concentration c_0. The viscosity at this concentration for the electrolyte is taken from the literature[64]. With these crude but reasonable approximations, only ζ potential (a measure of the surface charge of the capillary) is fitted to the experimental data for the apparent diffusivity, extracted from the experimental Sand's time in the main text.
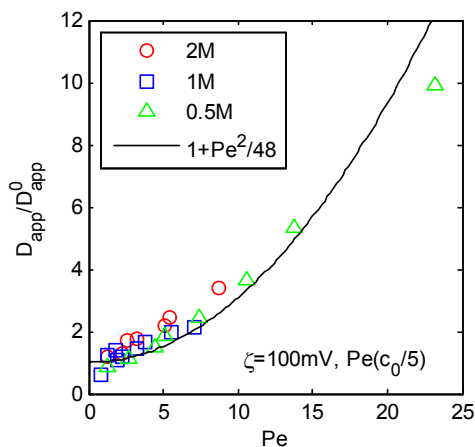
Figure S4. Comparison of the D_{app} obtained from the capillary cells with the Taylor dispersion formula.

Table S3. Parameters used for the Taylor dispersion formula.

c_0 (mol l^{-1})	ϵ_r	ζ (mV)	$^a\eta$ [64] (mPa s)	$^a\sigma_0$ [42] (mS cm^{-1})	D^0_{app} (cm^2 s^{-1})	D_0 [42] (cm^2 s^{-1})	t_{Li} [42]
0.5	35	100	1.35	2.5	0.5×10^{-6}	3.4×10^{-6}	0.38
1	35	100	1.53	4.6	0.7×10^{-6}	3.0×10^{-6}	0.38
2	35	100	2.00	7.7	0.4×10^{-6}	1.7×10^{-6}	0.38

^{a}Evaluated at $c_0/5$.

This simple theory leads to a reasonable collapse of the experimental data for hydrodynamic dispersion versus Peclet number, as shown Fig. S4. The scaling function lies close to the prediction of Taylor dispersion in the EO vortices observed near the tips. Despite some admittedly very rough approximations, the analysis shows that the observed scaling with current, departing from the classical Sand's formula based on linear diffusion alone, could be attributable

to hydrodynamic dispersion resulting from EO flow in the capillary. This is also consistent with our direct observations of the flow.

An important observation is that the data collapse extrapolates to an apparent diffusivity at zero current that is consistent with literature values for this electrolyte. This means that the results of our capillary experiments, which show noticeable effects of convection at high currents, also have relevance for practical batteries, where EO flow may be negligible. As shown in the main text, the main difference with a theory based purely on diffusion is that the experimentally observed scaling with current is different in the capillary cell. The sandwich cell results (also without significant convection) further confirm the validity of the predicted mechanisms of lithium growth determined by direct visualization in the capillary cell.

Blockage versus penetration of lithium deposits in sandwich cells
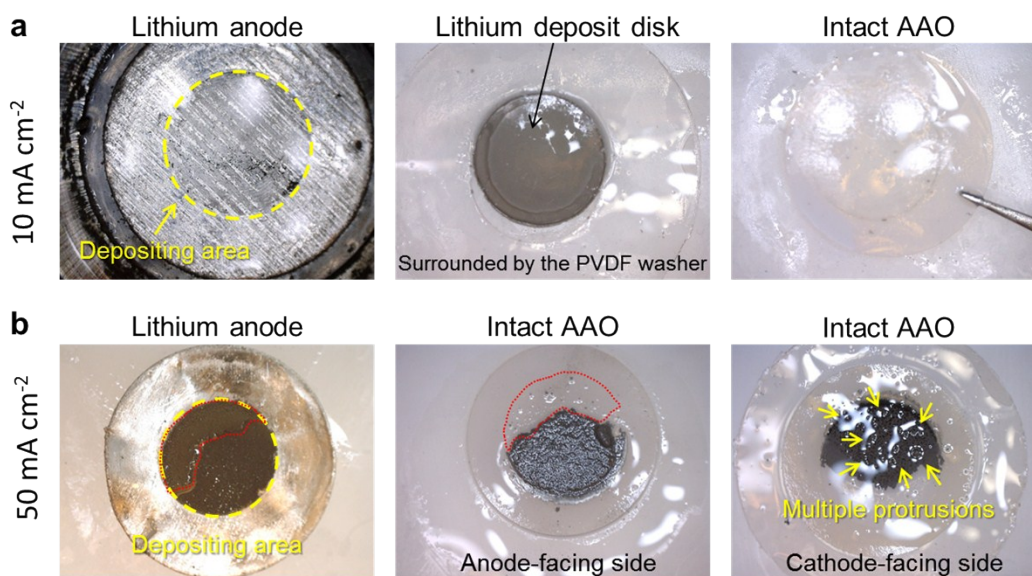
Figure S5. Digital photos of the lithium electrodes, deposits and anodic alumina oxide (AAO) separators harvested from the sandwich cells experiments shown in Fig. 3. In contrast to the clear AAO (a), penetration of AAO by lithium deposits is clearly visible in the case of overlimiting-current deposition (b).

Derivation of the scaling function $f(\tilde{J})$ for the dilute binary electrolyte

Methods of solving diffusion equations can be found in many text books on transport phenomena. Here, we provide an example of derivation to get the scaling function $f(\tilde{J})$.

In a dilute binary electrolyte, the single salt dissociates into equal numbers of anions and cations, i.e. $c_a=c_c=c$, with the charge numbers $z_c=-z_a=1$. Neglecting the convection, the evolution of the concentrations in a one-dimensional system can be modeled by the following set of equations[21],

$$\frac{\partial c}{\partial t} = D_a \frac{\partial^2 c}{\partial x^2} + z_a \mu_a F \frac{\partial}{\partial x}\left(c \frac{\partial \phi}{\partial x} \right) \qquad \text{(S2)}$$

$$\frac{\partial c}{\partial t} = D_c \frac{\partial^2 c}{\partial x^2} + z_c \mu_c F \frac{\partial}{\partial x}\left(c \frac{\partial \phi}{\partial x} \right) \qquad \text{(S3)}$$

where D_i and μ_i are diffusion coefficient and mobility of either the anions or the cations, ϕ is the potential applied to the system to maintain the required current density. Elimination of the potential terms yields an effective diffusion equation[21],

$$\frac{\partial c}{\partial t} = D_{app} \frac{\partial^2 c}{\partial x^2}, \quad \text{with} \quad D_{app} = \frac{z_c \mu_c D_a - z_a \mu_a D_c}{z_c \mu_c - z_a \mu_a} \qquad \text{(S4)}$$

By using the Nernst-Einstein relation, $D_i = RT\mu_i$, we can rewrite the effective diffusivity D_{app} and the transference number as,

$$D_{app} = \frac{2 D_c D_a}{D_c + D_a} \qquad \text{(S5)}$$

$$t_a = 1 - t_c = \frac{-z_a \mu_a}{z_c \mu_c - z_a \mu_a} = \frac{D_a}{D_c + D_a} \qquad \text{(S6)}$$

so that $D_{app}=2D_c t_a=2D_a t_c$.
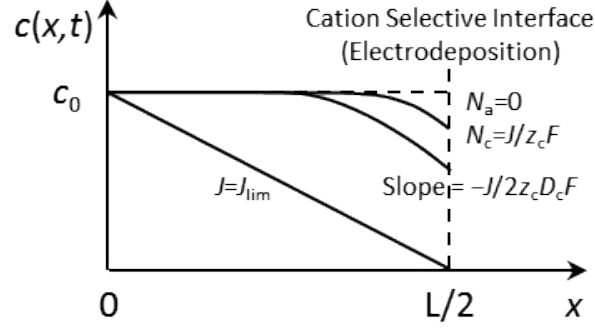
Figure S6. Concentration evolution in the diffusion layer near the surface of the electrode.

We are interested in the concentration evolution near the surface of the electrode when an overlimiting current is applied. From the fact that the current at the boundary ($x=L/2$) is contributed solely by the electrodeposition of cations, we have the flux of anions as

$$0 = N_a\big|_{x=L/2} = -z_a \mu_a F c \frac{\partial \phi}{\partial x} - D_a \frac{\partial c}{\partial x} \tag{S7}$$

Therefore, the flux of cations at $x=L/2$ is

$$\frac{J}{z_c F} = N_c\big|_{x=L/2} = -z_c \mu_c F c \frac{\partial \phi}{\partial x} - D_c \frac{\partial c}{\partial x} = -2D_c \frac{\partial c}{\partial x} \tag{S8}$$

from which one can define the limiting current as,

$$J_{\lim} = 2z_c F D_c \frac{c_0}{L/2} = \frac{4 z_c c_0 F D_c}{L} = \frac{2 z_c c_0 F D_{app}}{t_a L} \tag{S9}$$

We can then use Eqs (S8) and (S9) to obtain the dimensionless boundary condition by scaling c to c_0, x to $L/2$ and t to $(L/2)^2/D_{app}$,

$$\frac{\partial \tilde{c}}{\partial \tilde{x}} = -J \Big/ \frac{2 z_c c_0 F D_{app}}{t_a L} = -J/J_{\lim} = -\tilde{J} \tag{S10}$$

To solve the time it takes to deplete the concentration at the surface of the electrode to zero when an overlimiting current is applied, we construct

$$\tilde{c}(\tilde{x}, \tilde{t}) = -\frac{1}{\tilde{J}} \frac{\partial \tilde{c}}{\partial \tilde{x}} \tag{S11}$$

which should satisfy the linear ambipolar diffusion equation (S4)

9

$$\frac{\partial \tilde{u}}{\partial \tilde{t}} = \frac{\partial^2 \tilde{u}}{\partial \tilde{y}^2} \tag{S12}$$

where we have applied $\tilde{y} = 1-\tilde{x}$.

With the following initial and boundary conditions,

$$\tilde{u}(\tilde{y},\tilde{t}=0)=0; \quad \tilde{u}(\tilde{y}=0,\tilde{t})=1 \tag{S13}$$

the dynamics is governed by the complementary error function (erfc) [55],

$$\tilde{u} = \mathrm{erfc}\left(\frac{\tilde{y}}{2\sqrt{\tilde{t}}}\right) \tag{S14}$$

So that,

$$\frac{\partial \tilde{c}}{\partial \tilde{x}} = -\tilde{J}\,\mathrm{erfc}\left(\frac{1-\tilde{x}}{2\sqrt{\tilde{t}}}\right) \tag{S15}$$

Integration of Eq (S15) and application of the initial and boundary conditions in Eq (S13) yield

$$\tilde{c}(\tilde{x},\tilde{t}) = 1 - 2\sqrt{\tilde{t}}\,\tilde{J}\,\mathrm{ierfc}\left(\frac{1-\tilde{x}}{2\sqrt{\tilde{t}}}\right) \tag{S16}$$

where the iterated integral of complementary error function (ierfc) is defined as,

$$\mathrm{ierfc}(z) = \int_z^\infty \mathrm{erfc}(z)\,dz$$

$$\mathrm{erfc}(z) = \frac{2}{\pi}\int_z^\infty e^{-s^2}\,ds \tag{S17}$$

For $\tilde{J} > 1$, the Sand's time can be solved via Eq (S16) at zero concentration,

$$\tilde{c}(\tilde{x}=1,\tilde{t}=\tilde{t}_{Sand}) = 1 - 2\sqrt{\tilde{t}_{Sand}}\,\tilde{J}\,\mathrm{ierfc}(0) = 0 \tag{S17}$$

Using ierfc$(0) = \pi^{-0.5}$, the final form of the scaling function is obtained,

$$\tilde{t}_{Sand} = f_{dilute}\left(\tilde{J}\right) = \frac{\pi}{4\tilde{J}} \tag{S18}$$

Capillary cell experiments with ether-based electrolytes
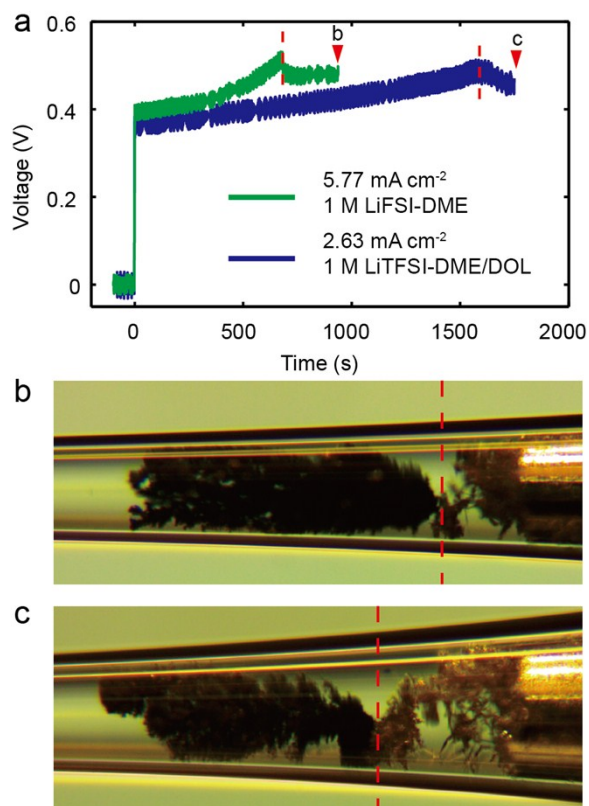
Figure S7. Transition from mossy lithium (collection of root-growing whiskers) to tip-growing fractal lithium in ether-based electrolytes. (a) Voltage responses of the constant-current electrodepositions. Final snapshots of lithium deposits in (b) 1 M LiFSI-DME electrolyte and (c) 1 M LiTFSI-DME/DOL electrolyte. Corresponding movies S6 and S7 are available in the online electronic supplementary information. While the dynamics are similar to those in carbonate-based electrolytes, the differences in the appearance are attributable to the different SEI layers formed in ether-based electrolytes.

References (continued)

63.   A. Yaroshchuk, E. Zholkovskiy, S. Pogodin, V. Baulin, *Langmuir* **27** 11710 (2011).

64.   Y. R. Dougassa, J. Jacquemin, L. El Ouatani, C. Tessier, M. Anouti, *The Journal of Physical Chemistry B* **118** 3973 (2014).